Highly pathogenic avian influenza H5N8 in south-west France 2016–2017: A modeling study of control strategies

Alessio Andronico, Aurélie Courcoul, Anne Bronner, Axelle Scoizec, Sophie Lebouquin-Leneveu, Claire Guinat, Mathilde C Paul, Benoît Durand, Simon Cauchemez

Highly pathogenic avian influenza H5N8 in south-west France 2016–2017: A modeling study of control strategies

Alessio Andronico[a,*], Aurélie Courcoul[b,1], Anne Bronner[c], Axelle Scoizec[d], Sophie Lebouquin-Leneveu[d], Claire Guinat[e], Mathilde C. Paul[e], Benoît Durand[b], Simon Cauchemez[a]

[a] Mathematical Modelling of Infectious Diseases Unit, Institut Pasteur, UMR2000, CNRS, 75015, Paris, France
[b] Epidemiology Unit, Paris-Est University, Laboratory for Animal Health, French Agency for Food, Environment and Occupational Health and Safety (ANSES), Maisons-Alfort, France
[c] Direction générale de l'Alimentation, Paris, 75015, France
[d] Anses, Laboratoire de Ploufragan-Plouzané, Unité d'épidémiologie et bien-être en aviculture et cuniculture, Ploufragan, 22440, France
[e] IHAP, Université de Toulouse, INRA, ENVT, Toulouse, France

ARTICLE INFO

ABSTRACT

In the winter 2016–2017 the largest epidemic of highly pathogenic avian influenza (HPAI) ever recorded in the European Union spread to all 28 member states. France was hit particularly hard and reported a total of 484 infected premises (IPs) by March 2017. We developed a mathematical model to analyze the spatiotemporal evolution of the epidemic and evaluate the impact of control strategies. We estimated that farms rearing ducks were on average 2.5 times more infectious and 5.0 times more susceptible to HPAI than farms rearing other avian species. The implementation of surveillance zones around IPs reduced transmission by a factor of 1.8 on average. Compared to the strengthening of pre-emptive culling measures enforced by French authorities in February 2017, we found that a faster depopulation of diagnosed IPs would have had a larger impact on the total number of infections. For example, halving the time delay from detection to slaughter of infected animals would have reduced the total number of IPs by 52% and total cull numbers by 50% on average. This study showcases the possible contribution of modeling to inform and optimize control strategies during an outbreak.

1. Introduction

Outbreaks of Highly Pathogenic Avian Influenza (HPAI) have been reported since 1959 and have caused considerable socioeconomic damages on poultry farming in affected areas (Alexander, 2000). In addition to the impact on animal health and welfare, HPAI outbreaks also constitute a potentially serious threat for humans due to the possible emergence of a new pandemic strain after genetic reassortment in mammalian hosts (Peiris et al., 2007; Smith et al., 2009).

In the winter 2016–2017 an epidemic of HPAI - HPAI H5 clade 2.3.4.4, mainly subtype H5N8 - hit the European Union (EU) and was the largest ever recorded in the EU in terms of number of outbreaks and geographical extent. After a first case in wild birds was reported in Hungary on 1 November 2016, the epidemic wave quickly reached the other 27 European countries (Brown et al., 2017). France, and in particular its south-west region with a high density of foie gras producers,

was hit particularly hard and reported a total of 484 infected premises (IPs) by March 2017 (Bronner et al., 2017). Control measures were implemented right after the start of the epidemic. However, despite the implementation of reinforced control measures on 2 February 2017, the epidemic persisted. A 6-week ban on duck movements entering the affected area was implemented from 17 April 2017 to 28 May 2017. This resulted in a progressive depopulation of the affected area as farmers were only allowed to send their ducks to slaughter but not to introduce new flocks onto their farms, and it also allowed for a deep sanitization of the holdings of all actors involved in their production (farmers, veterinarians, and trucking companies) (Arrêté du 31 mars, 2017). The last infected premise was detected on 23 March 2017 and the control measures were lifted on 29 May 2017 (Bronner et al., 2017). Since then, no other HPAI outbreak has been reported in France.

While no human cases were observed, the control policies that were enacted in France during the 2016–2017 epidemic resulted in the

culling of about 6.8 million poultry and induced severe perturbations to poultry production, causing important economic losses for local producers and for the whole poultry sector (Guinat et al., 2018) as well as the closure of some export markets. In this context, it is important to gain a deeper mechanistic understanding of the disease dynamics and to develop tools to assess, refine, and tailor control strategies, which could thus help to control HPAI transmission and limit its disruptive impact on poultry trade should a new outbreak occur.

In this paper we developed a mathematical model to analyze the spatiotemporal evolution of the epidemic and evaluate the impact of control strategies on the epidemic dynamics. Drawing from previous work on Foot and Mouth Disease (FMD) (Chis Ster and Ferguson, 2007; Ferguson et al., 2001; Keeling et al., 2001), and HPAI in the Netherlands (Le Menach et al., 2006) and in Southeast Asia (Walker et al., 2012, 2010), our model captured how the risk of infection varied with time and distance for different farm types, while also taking into account the effect of control measures implemented once IPs were detected. While a previous study of the H5N8 epidemic in France focused on the spatiotemporal clustering of duck-rearing IPs (Guinat et al., 2018), our analysis was informed by data on all IPs detected in the south-west of France during the 2016–2017 epidemic.

2. Materials and methods

2.1. Data and preprocessing

Three datasets were used to calibrate our model. The first one included the list of 471 HPAI IPs detected between 28 November 2016 and 23 March 2017 in the south-west of France, and containing information on the farm production type, geographical coordinates, identifier, and dates of suspicion, symptom onset (when available), and of culling. Twenty-eight IPs had an ambiguous or missing identifier and were therefore excluded from the analyses, leaving us with 443 IPs. The second dataset included identifier and culling date for 461 preventively culled farms. Except for 5 farms, we had no data on preventive culling measures concerning farms rearing poultry other than ducks. The final dataset consisted of information (identifier, geographical coordinates, municipality, department, and type) on all commercial farms of poultry within 100 km from an IP, covering 17 departments in the south-west region of France. After merging holdings belonging to the same owner and separated by less than 250 m, we were left with a total of 8380 farms. 1421 farms (17%) in this dataset had coordinates corresponding to the centroid of the municipality in which they are located. In such cases, we reassigned their coordinates by randomly drawing points within that same municipality. In a sensitivity analysis described in Supplement 1, we show that this preprocessing step did not affect inference.

We assigned to each farm one of two labels according to the type of species they reared: 1) galliformes (for farms raising chickens, hens, quails, and turkeys) and 2) palmipeds (for farms raising ducks and geese). Eight percent of farms (694/8380) reared both species and were classified as palmipeds, since the latter represented the vast majority (395/443 = 89%) of IPs. In total there were 4189 galliformes (50%) and 4191 palmipeds farms in our final dataset. Three types of production were distinguished for palmipeds: rearing (1-day old ducklings are reared for around 3 weeks), breeding (3-week old ducks are reared for around 9 weeks) and force-feeding (12-week old ducks are force-fed for around 12 days).

2.2. Control measures

Following European directives, once an IP was notified, its stamping out was planned and movement restrictions, surveillance and biosecurity were enforced in a 10-km radius around the IP (surveillance zone) - with additional constraints (e.g. pre-emptive culling, active surveillance in all poultry farms with visits for clinical inspection and
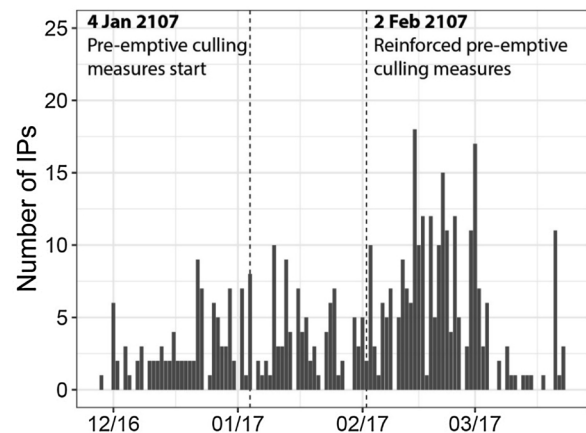

Fig. 1. Epidemic curve. Daily number of IPs by date of suspicion.

sampling for virus detection in palmipeds farms, transit ban for all vehicles related to poultry farming except on highways, and ban of game birds hunting) in a 3-km radius around the IP (protection zone).

Pre-emptive culling measures in the protection zones started on 4 January 2017 (Bronner et al., 2017) and were reinforced from 2 February 2017. They targeted 1) all poultry farms within 1 km from an IP, irrespective of their production type (galliformes or palmipeds); and 2) duck breeding farms within 3 km from an IP.

Fig. 1 shows the epidemic curve and highlights the key dates relating to control measures. The first IP was notified on 28 November 2016 in the Tarn department. The daily number of IPs remained quite stable until the end of January 2017 when a clear increase was observed: this second wave was mainly characterized by transmission events occurring in the Landes department (see Figure S2).

2.3. Mathematical model

We developed a space-time survival model in which the daily force of infection experienced at time t by susceptible farm j is given by:

$$\lambda_j(t) = \sum_i \lambda_{i \to j}(t) \cdot I \left[i \text{ infectious at } t \right] + \lambda_j^{ext} \tag{1}$$

where I is the indicator function, $\lambda_{i \to j}(t)$ is the force of infection that farm i exerts on j at time t, and λ_j^{ext} is an external term accounting for infection sources other than IPs - e.g. the presence of infectious wild birds or backyard poultry.

For $\lambda_{i \to j}(t)$ we assumed a frequency-dependent functional form:

$$\lambda_{i \to j}(t) = \psi_i \cdot \phi_j \cdot \alpha_{SZ}(i, j, t) \cdot \frac{\beta(t)}{N_i(d_c)} \cdot I(d_{ij} \leq d_c) \tag{2}$$

where ψ_i is the relative infectivity of i (with $\psi_i = 1$ for palmipeds and $\psi_i = \psi$ for galliformes farms), ϕ_j is the relative susceptibility of j (with $\phi_i = 1$ for palmipeds and $\phi_i = \phi$ for galliformes farms), $\alpha_{SZ}(i, j, t)$ is a multiplicative term accounting for changes in transmission in the surveillance zones, $\beta(t)$ is the transmission rate, d_c is a cutoff distance, $N_i(d_c)$ is the number of farms within distance d_c from i, and d_{ij} is the distance between farms i and j. This choice of functional form for the force of infection assumes that transmission between farms was only possible for distances below d_c and that each IP had a fixed number of contacts, irrespective of the number of farms around it.

The term $\alpha_{SZ}(i, j, t)$ was defined as:

$$\alpha_{SZ}(i, j, t) = \begin{cases} \alpha_{SZ} & \text{if } i \text{ or } j \text{ are in a surveillance zone at time } t \\ 1 & \text{otherwise} \end{cases} \tag{3}$$

In other words, we assumed that if either one of the farms in contact - i or j in Eq. (3) – happened to be in a surveillance zone at time t, all the measures implemented therein (movement restrictions, active surveillance, and biosecurity) would result in a change of transmission rate.

We tested different functional forms for the transmission rate $\beta(t)$ (Supplement 2), but the one providing the best fit to the data was a stepwise transmission rate with two switch points (t_1 and t_2) for the Landes department:

$$\beta(t) = \begin{cases} \beta_1 & \text{if } t < t_1 \\ \beta_2 & \text{if } t_1 \leq t < t_2 \\ \beta_3 & \text{if } t \geq t_2 \end{cases} \tag{4}$$

and a constant transmission rate for all other departments.

The external force of infection was defined as:

$$\lambda_j^{ext} = \beta_{ext} \cdot \phi_j \tag{5}$$

In a sensitivity analysis described in Supplement 2 we considered alternative model formulations with 1) a constant transmission rates (no switch points); 2) one switch point; and 3) a density-dependent version of the model described above.

2.4. Inference

Our final dataset contained three different types of IPs: 1) farms where the owners reported unusual deaths or symptomatic birds and that were later confirmed as infected (IPs detected by passive surveillance, 193/443 = 44% of total IPs); 2) preventively culled IPs (134/443 = 30% of total IPs); 3) IPs detected by active surveillance before symptom onset (113/443 = 26% of total IPs).

We assumed that, following infection, IPs detected by passive surveillance were latent for L days and had an incubation period of T days prior to developing symptoms. We also assumed a fixed delay of D days between infection and culling (for preventively culled IPs) and between infection and suspicion (for IPs detected by active surveillance). This allowed us to infer, for each IP, the time of infection, which, in practice, was unobserved. Fig. 2 schematically shows the three types of IPs.

Once the times of infection were assigned, the probability of farm j being infected on day τ_j, conditional on having avoided infection until that day, could be computed as:

$$p_j^I = 1 - \exp[-\lambda_j(\tau_j)] \tag{6}$$

Similarly, the probability of farm j escaping infection until τ_j - 1 was:
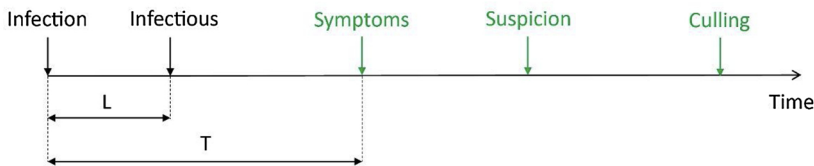
Table 1

Estimates of model parameters for the best fitting model (latent period $L = 1$ day, incubation period $T = 7$ days, delay between infection and preventive culling or detection $D = 5$ days, and cutoff distance $d_c = 15$ km).

Parameter	Mean	95% CI
ψ: Relative infectivity of galliformes farms	0.39	0.10, 0.85
ϕ: Relative susceptibility of galliformes farms	0.20	0.15, 0.27
α_{SZ}: Effect of surveillance zones on transmission rate	0.58	0.42, 0.80
β_0: Transmission rate (all departments except for Landes)	0.23	0.16, 0.31
β_1: Transmission rate in Landes department (28 Nov 2016 - 22 Jan 2017)	0.31	0.20, 0.47
β_2: Transmission rate in Landes department (23 Jan 2017 - 11 Feb 2017)	0.53	0.37, 0.72
β_3: Transmission rate in Landes department (12 Feb 2017 - 14 Apr 2017)	0.28	0.18, 0.40
β_{ext} (10^{-4}): External transmission rate	0.86	0.62, 1.15

$$p_j^E = \exp\left[-\sum_{\tau=0}^{\tau_j-1} \lambda_j(\tau)\right] \tag{7}$$

From Eqs. (6) and (7), the likelihood function could be evaluated for any set of model parameters. We used the algorithm described in (Cauchemez and Ferguson, 2012) to speed up computations.

The model parameters (the relative susceptibility and infectivity, the transmission rates, and the effect of surveillance zones on transmission) are listed in Table 1 and were estimated using Markov Chain Monte Carlo (MCMC) sampling (Gilks et al., 1996) with flat priors. Chain convergence was assessed by visual inspection of the traceplots.

The inference procedure was repeated for a large number of models differing in the choice of switch points t_1 and t_2, cutoff distance d_c, and time intervals L, T, and D (see Supplement 3). The Deviance Information Criterion (DIC) was used for model selection (Gelman et al., 2014).

Delays in detection, culling, and preventive culling were fitted to Gamma distributions (Supplement 4) that were used when simulating the alternative control strategies described below. Similarly, empirical distribution functions obtained from data (Supplement 5) were used for simulating the proportion of farms preventively culled around IPs.

1. IPs detected by passive surveillance

2. Preventively culled IPs

3. IPs detected by active surveillance

Fig. 2. Time intervals needed to evaluate the likelihood function. L represents the latent period, T the incubation period, and D the time interval from infection to culling (suspicion) for IPs that were preventively culled (detected by active surveillance), respectively. Green denotes observed dates while black denotes unobserved time points (For interpretation of the references to colour in this figure legend, the reader is referred to the web version of this article).

2.5. Simulations

The same framework used for inference was then employed to simulate epidemic scenarios under different control measures. Using Eqs. (6) and (7) with parameters drawn from the posterior distribution, it was possible to compute the probability of infection for each farm at each time step and simulate multiple epidemics while also keeping track of the transmission tree (i.e. which IP infected which farm).

We thus studied the effect of five main variables: 1) the choice of culling radius; 2) the type of farms targeted by the pre-emptive culling measures; 3) the time delay in stamping out an IP once detected; 4) the time delay in carrying out preventive culling around detected IPs; and 5) the radius of the movement restrictions zones (i.e. the surveillance zones).

While we assumed that the parameters of our model were the same for ducks and geese farms, when simulating preventive culling measures, we did differentiate between duck-rearing versus other palmiped farms.

To allow for a direct comparison to the real epidemic, all simulations were stopped at the beginning of the 6-week ban on duck movements (14 April 2017), i.e. three weeks after the last IP was reported.

3. Results

3.1. Parameter estimates and goodness of fit

The model that better supported by the data had a latent period $L = 1$ day, incubation period $T = 7$ days, a delay between infection and preventive culling or detection $D = 5$ days, and a cutoff distance $d_c = 15$ km. According to this model, transmission was constant in all departments but the Landes, for which two switch points provided the best fit: $t_1 = 23$ January 2017 and $t_2 = 12$ February 2017 (see Supplement 3).

Table 1 shows the estimates of model parameters.

We found that the infectivity and susceptibility of galliformes farms was only 39% (Credible Interval (CI): 10%–85%) and 20% (CI: 15%–27%) of that of palmipeds farms, respectively.

The model also estimated that transmission in the surveillance zone was reduced by $1 - \alpha_{SZ} = 42\%$ (CI: 20%–58%), confirming the relevance of the control measures (active surveillance, movements restrictions) implemented in the surveillance zones around IPs in order to contain disease spread.

Fig. 3 shows the estimated transmission rates through time: the best fitting model shows an increase of transmission in the Landes
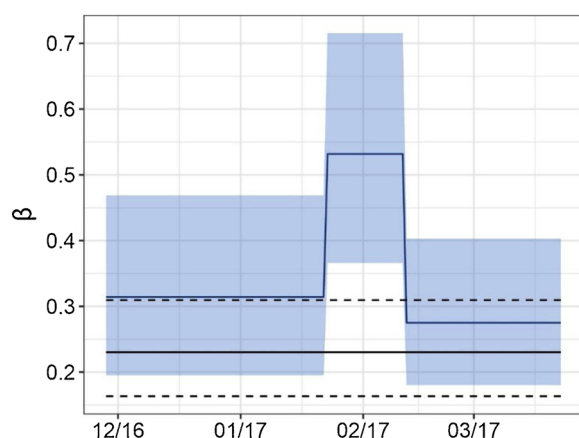

Fig. 3. Transmission rate through time. Blue: transmission rate in the Landes department. Black: transmission rate in the other departments. Solid lines denote averages while the shaded region and the dashed lines denote the 95% CI (For interpretation of the references to colour in this figure legend, the reader is referred to the web version of this article).

department between the end of January and the first weeks of February 2017. This period corresponds to the beginning of the second epidemic wave hitting that department right before the implementation of reinforced pre-emptive culling on 2 February 2017.

From the reconstructed transmission trees, we looked at temporal variations of reproduction number and infection distance (Fig. 4). The average reproduction number was slightly above one for the first part of the epidemic but quickly rose above 1.5 as the second epidemic wave (Fig. 4A) hit the region and in particular the Landes department (Figure S2). The infection distance was quite stable around its overall average - 8.5 km (CI: 8.2 km–8.8 km) - but showed a clear decrease right before the second epidemic wave.

Palmipeds IPs were the main drivers of the epidemic: 84% (CI: 79%–87%) of all transmission events were due to palmipeds IPs, only 5% (CI: 1%–9%) were due to galliformes IPs, and 11% (CI: 10%–13%) to the external transmission rate. Most - 58% (CI: 54%–62%) - transmission events occurred within 10 km from an IP.

The model was able to accurately reproduce the epidemic dynamic globally and at the department level (Fig. 5, Figure S3, and Figure S4).

According to the DIC, alternative model formulations with a constant transmission rate or with only one switch point were not equally well supported by the data. Similarly, density-dependent variants of the model had higher DICs than our baseline model (Supplement 2).

3.2. Control measures

Table 2 shows the complete summary of all the scenarios we considered.

3.2.1. Preventive culling radius

The preventive culling strategy implemented on 2 February 2017 targeted all poultry farms within 1 km from an IP and all duck breeding farms within 3 km from an IP. Here we simulated alternative control strategies targeting all farms within x km from an IP, with x going from 0 km (no preventive culling) to 5 km, and starting on 4 January 2016 (i.e. on the first date preventive culling measures were implemented in reality).

While a 1 km preventive cull halves the total number of IPs compared to no preventive cull, the marginal benefits of further increasing the intervention area are only relatively limited (Fig. 6). For example, when the preventive culling radius is 5 km the model still predicts an average of 286 IPs (versus 1027 IPs with no preventive culling and 502 IPs with 1 km preventive culling), while the expected number of preventively culled farms is 1122 farms (CI: 5–1638) - corresponding to approximately 13% of all the farms in our dataset (this number is 329 farms (CI: 19–545) when the preventive culling radius is 1 km).

3.2.2. Type of farms concerned by the preventive culling measures

The second set of simulations aimed at assessing the effect of targeting the preventive culling measures to different types of farms. Starting from our baseline model (preventive culling measures concerning all poultry farms within 1 km and all duck breeding farms within 3 km from an IP), we considered two alternative strategies targeting 1) only palmipeds farms within 1 km and duck breeding farms within 3 km from an IP; and 2) only duck breeding farms within 3 km from an IP. As shown in Table 2, while the first strategy results in a reduction (8%) of the total number of preventively culled farms (482 vs 526) with approximately the same total number of IPs (411 vs 408), the second strategy is associated to a considerably (44%) larger epidemic (587 vs 408 IPs).

3.2.3. Stamping out delay

During the course of the epidemic, the average delay from the detection of an IP to the slaughter of its animals was $d_S = 5.2$ days (see Supplement 4). We simulated two alternative scenarios representing 1) faster stamping out ($d_S = 2$ days); and 2) slower stamping out ($d_S = 10$
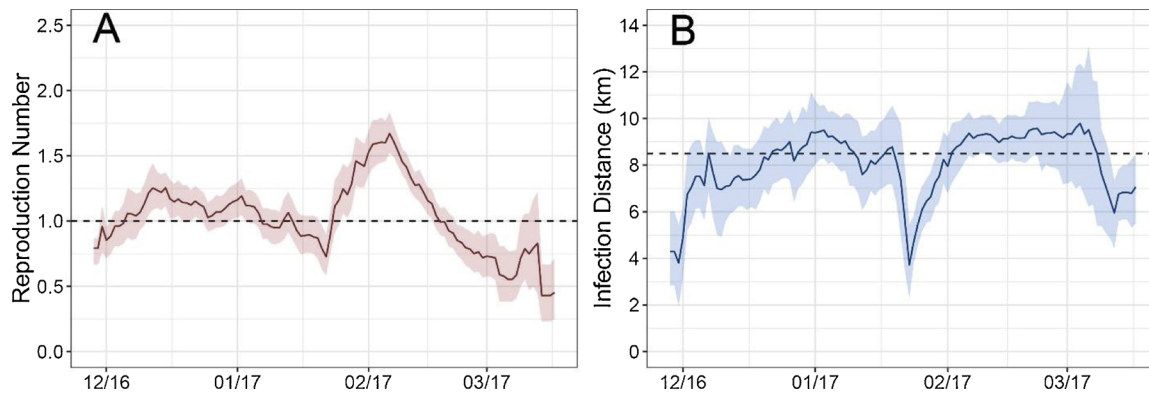
Fig. 4. Reproduction number (A) and infection distance (B) through time. Colored lines represent averages while colored areas represent 95% CIs. Moving average smoothing with a window of 1 week was used to improve clarity. The dashed curve in panel A corresponds to a reproduction number of 1, while the dashed line in panel B corresponds to the average distance calculated over the entire epidemic (8.5 km).
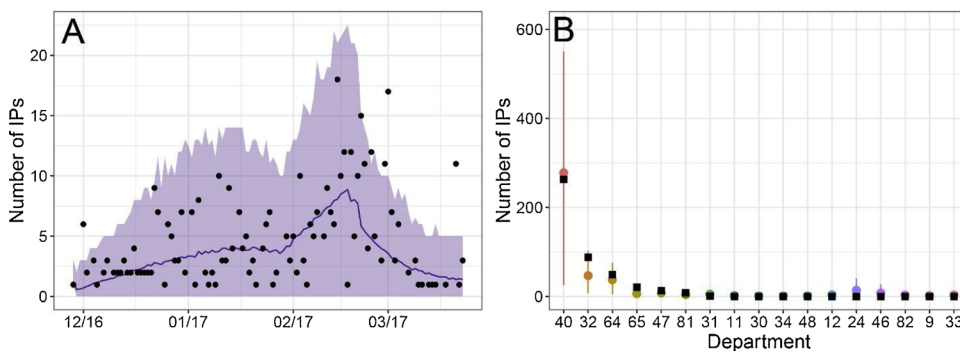
Fig. 5. Goodness of fit. A. Daily number of IPs through time by date of suspicion. Simulations from the model are in purple: the solid line corresponds to the average while the shaded region corresponds to the 95% CI. Black dots represent data. B. Total number of IPs by department. Simulations from the model are shown in color: dots represent averages while lines represent 95% CIs. Black squares represent data (For interpretation of the references to colour in this figure legend, the reader is referred to the web version of this article).

days). As expected, d_S has a large effect on the epidemic dynamics: in particular we found that its effect on the number of IPs is approximately linear. If $d_S = 2$ days, the total number of IPs is reduced by a factor close to 2 with respect to our baseline scenario (196 vs 408 IPs). On the other hand, for $d_S = 10$ days, the number of IPs increases by a factor close to 2 (783 vs 408 IPs).

3.2.4. Preventive culling delay

The average delay from detection of an IP to the preemptive culling of neighboring farms was $d_P = 7.8$ days. Similarly to the previous set of simulations, we studied two alternative scenarios corresponding to 1) faster preventive culling measures ($d_P = 4$ days); and 2) slower preventive culling measures ($d_P = 16$ days). As seen in Table 2, both alternative strategies have only a modest effect on the total number of IPs.

3.2.5. Surveillance zone radius

The last set of simulations aimed at studying the effect of the size of surveillance areas, i.e. the zones where movement restrictions and active surveillance are enforced. Starting from the baseline value of 10 km for the surveillance radius we simulated two alternative strategies with 1) a radius of 5 km and 2) a radius of 15 km. Both strategies had a moderate impact on the epidemic size (see Table 2).

4. Discussion

In this paper we analyzed a large outbreak of HPAI subtype H5N8 that took place in the south-west of France from the end of November 2016 to March 2017. We developed and calibrated a mathematical model that was able to accurately capture and reproduce the dynamics of the outbreak. This allowed the estimation of key epidemiological parameters such as the relative susceptibility and infectivity of the different farm types, the transmission rate through time, and the effect

of surveillance zones on transmission. We subsequently used our model to evaluate the effect of different culling strategies. Our results indicate that a quicker depopulation of diagnosed IPs would have impacted the total number of infections more effectively than reinforcing pre-emptive culling measures around IPs. In particular, halving the time delay from IP detection to its stamping out would have reduced IPs by 52% and total cull numbers by 50% on average. This result is consistent with previous studies on HPAI and FMD (Ferguson et al., 2001; Keeling et al., 2001; Le Menach et al., 2006). Since culling protocols are much more strict, complex, and cumbersome for stamping out IPs (slaughter performed on breeding sites by a veterinarian or by authorized personnel, reinforced biosecurity and disinfection measures…) than for pre-emptive culls (performed at slaughterhouses), our results suggest that emergency plans for future HPAI crises should focus on allocating appropriate human and material resources with the aim of minimizing as much as possible stamping out delays for IPs.

We found that the model with better support from the data was a frequency-dependent model where each IP had a fixed number of contacts and where transmission could only occur for distances within 15 km from an IP. With this model, the mean transmission distance was estimated at 8.5 km, consistent with a previous study based on spatio-temporal clustering of duck-rearing IPs (Guinat et al., 2018). These findings suggest that most transmission events occurred possibly through movement of animals, materials, or personnel between farms, rather than through animal contact or airborne spread - the latter being unlikely to play a role for this range of distances (Spekreijse et al., 2011). Additionally, the external transmission rate - capturing the effect of wild avifauna and backyard poultry - accounted for only 11% of infections, suggesting that the main driver of the epidemic was farm-to-farm transmission.

We found that transmission varied through time in Landes but not in other departments (Supplement 2). Transmission was also higher from the end of January to mid-February 2017. Even though Landes is the

Table 2

Summary of the alternative pre-emptive culling strategies explored via simulation studies. The different columns represent the total number of IPs, the number of departments with at least one IP, the number of municipalities with at least one IP, the total number of preventively culled farms, the number of preventively culled palmipeds farms, the number of preventively culled galliformes farms, the number of IPs detected by passive surveillance, the number of preventively culled IPs, and the number of IPs detected by active surveillance. The first row summarizes the observed epidemic, while the second row (baseline) corresponds to the main model described in the text. Each simulation entry reports the average and the 95% CI.

|	IPs	Departments	Municipalities	Preventively culled	Preventively culled (palmipeds)	Preventively culled (galliformes)	Passive surveillance	Preventively culled IPs	Active surveillance
Data	443	7	222	461	456	5	196	134	113
Baseline	408 [107, 753]	11 [8, 14]	234 [97, 348]	526 [113, 782]	482 [104, 708]	44 [8, 84]	180 [42, 330]	143 [29, 269]	86 [20, 154]
No preventive culling	1027 [333, 1440]	12 [9, 14]	373 [208, 501]	0 [0, 0]	0 [0, 0]	0 [0, 0]	644 [210, 905]	0 [0, 0]	383 [132, 551]
Culling radius 1 km	502 [46, 913]	11 [7, 14]	250 [43, 359]	329 [19, 545]	273 [16, 448]	56 [4, 105]	220 [22, 405]	163 [14, 293]	119 [10, 214]
Culling radius 2 km	414 [6, 750]	11 [4, 14]	234 [6, 345]	558 [2, 876]	444 [2, 687]	114 [1, 192]	182 [3, 335]	147 [2, 275]	85 [2, 155]
Culling radius 3 km	367 [93, 673]	12 [8, 14]	226 [84, 321]	785 [151, 1187]	611 [115, 904]	173 [35, 288]	162 [38, 305]	137 [32, 266]	67 [20, 122]
Culling radius 4 km	316 [30, 567]	11 [7, 14]	210 [28, 308]	964 [11, 1417]	737 [10, 1053]	227 [1, 359]	139 [11, 258]	122 [11, 230]	55 [6, 96]
Culling radius 5 km	286 [8, 567]	12 [6, 14]	200 [8, 309]	1122 [5, 1638]	848 [4, 1208]	274 [1, 439]	126 [4, 253]	114 [5, 236]	46 [1, 91]
Only palmipeds farms preventively culled	411 [16, 751]	11 [5, 14]	236 [15, 347]	482 [5, 713]	482 [5, 713]	0 [0, 0]	189 [7, 344]	129 [5, 245]	92 [3, 166]
Only duck breeding farms preventively culled	587 [4, 1001]	11 [2, 14]	288 [4, 421]	467 [1, 621]	467 [1, 621]	0 [0, 0]	330 [2, 555]	90 [1, 164]	167 [1, 280]
Stamping out delay 2 days	196 [4, 406]	11 [3, 14]	145 [4, 253]	263 [0, 528]	245 [0, 486]	19 [0, 42]	87 [2, 193]	64 [0, 136]	46 [1, 95]
Stamping out delay 10 days	783 [206, 1183]	12 [8, 14]	358 [163, 508]	849 [335, 1084]	760 [308, 974]	89 [21, 130]	341 [88, 518]	293 [75, 448]	149 [39, 227]
Preventive culling delay 4 days	376 [12, 659]	11 [5, 14]	226 [12, 336]	502 [4, 741]	461 [3, 670]	41 [1, 76]	165 [5, 293]	127 [4, 233]	84 [4, 147]
Preventive culling delay 16 days	457 [6, 817]	11 [4, 14]	242 [5, 358]	543 [2, 819]	494 [2, 730]	49 [1, 88]	200 [2, 367]	172 [2, 326]	85 [0, 151]
Surveillance radius 5 km	495 [4, 902]	11 [3, 14]	273 [4, 405]	597 [2, 853]	545 [1, 771]	52 [1, 90]	218 [2, 395]	173 [2, 308]	104 [1, 194]
Surveillance radius 15 km	363 [2, 700]	11 [2, 14]	211 [2, 320]	477 [1, 767]	437 [1, 689]	39 [0, 77]	160 [1, 314]	127 [1, 258]	76 [0, 145]
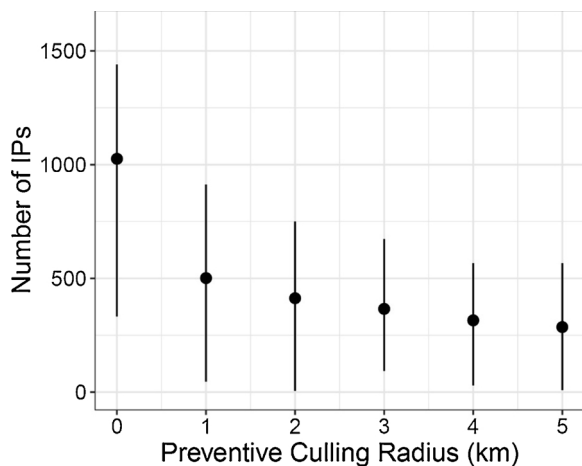
Fig. 6. Number of IPs for different preventive culling radius. The dots represent averages while the bars indicate the 95% CIs.

department with the highest density of commercial farms, models explicitly accounting for density-dependent effects alongside frequency-dependent transmission did not provide a good fit to the data (Supplement 2). Therefore, the estimated difference in transmission rate may be ascribed to the distinctive characteristics of the Landes department in terms of farming practices and environment. First, this department displays a considerable diversity of farming systems ranging from independent and small-size to very large integrated farms: official documents (French Ministry of Agriculture website, 2018) show that, compared to the other French departments, Landes exhibits the coexistence of diverse systems such as duck fattening and broiler (mainly free-range) production. Moreover, unlike neighboring departments, Landes has a high density of both ducks and chickens. Second, this department displays important heterogeneities in terms of biosecurity practices, as shown in a recent paper (Delpont et al., 2018): this study, based on 46 farms (22 located in the Landes department) identified three distinct clusters of farms based on 80 biosecurity measures. Significant variation was observed over the three clusters, including heterogeneity in managing the flow of people and vehicles, sharing of equipment, use of logbooks, handwashing, and cleaning and disinfection. Third, possible cases of noncompliance with governmental directives might also have played a role, but in absence of data documenting them, it is not possible to assess their potential impact on transmission dynamics. Finally, different environmental conditions could also have contributed to the estimated change in transmission rate: for example, large wetlands with a high density of wild avifauna characterize the Landes department (Eaufrance website, 2011) and, as a consequence, 38% of its municipalities are found in zones classified by the French government as being at high risk of HPAI outbreaks (Arrêté du 16 novembre, 2016).

We found that galliformes farms were less susceptible to infection than palmipeds farms, which is in line with recent studies on HPAI subtype H5N8 clade 2.3.4.4 (Bertran et al., 2016). Interestingly, our estimates indicate that galliformes farms were also less infectious in terms of viral shedding and accounted for only 5% of transmission events. If pre-emptive culling measures had targeted only palmipeds farms, the total number of IPs would have barely changed (from 408 to 411) but the total cull number would have reduced by 8% on average (Table 2).

The observation that the transmission rate in surveillance zones was approximately halved compared to non-surveillance zones (Table 1) indicate that control measures around IPs (such as preventive culling, active surveillance, and movement restrictions) are vital to contain disease spread.

This study has a number of limitations. First, our model implicitly

assumes that the epidemic was fully observed (100% reporting probability). Indeed, given the usually high mortality rate of HPAI it seems unlikely that clinically affected farms could have been missed. Moreover all the slaughtered flocks were tested for the presence of the virus, which allowed the detection of infected flocks where clinical signs were rare or absent. The surveillance of wild avifauna was also reinforced in the affected area, but only few positive animals were observed. In particular, none of 300 commensal wild birds living in or around outbreaks were found infected (Van De Wiele et al., 2017). Additionally, since we had no data on backyard poultry producers and smallholders, their possible effect on transmission is only indirectly captured through the β_{ext} parameter. Similarly, movements of animals were not explicitly included in the model although in practice, our cutoff distance d_c acts as a proxy for the average maximum movement distance. When data will become available, it would be interesting to extend our model to explicitly account for such effects. Our study also ignored the impact of within-farm epidemic dynamics and possible differences in biosecurity risks between small and large farms. The latter however should not have a major impact on the overall dynamics of the epidemic, which was well captured by the model (Fig. 5). Finally, our inference procedure relies on the deterministic assignment of time delays L, T, and D (Fig. 2), thus ignoring highly plausible differences between farms. This could be improved, at the expense of a considerably higher computational cost, by using data augmentation to infer individual time delays for each IP.

The approach we have developed provides a framework for estimating key parameters of HPAI outbreaks and, more importantly, for evaluating the impact of control strategies. While we have used it here retrospectively, this framework could also be used to provide real time estimates and forecast possible epidemic scenarios under different control strategies, thus providing useful inputs to inform policymakers' decisions.

Authors' contributions

AA, AC, BD, and SC designed the analyses. AB, AS, SL-L, CG, and MP provided the data and expertise on local epidemiology and control measures. AC and BD cleaned, merged, and reformatted the raw data. AA implemented the model, ran the analyses, and wrote the first draft of the manuscript. All authors discussed the results, contributed with comments and suggestions, and approved the final version of the manuscript.

Competing financial interests

The authors declare no competing financial interests.

Appendix A. Supplementary data

Supplementary material related to this article can be found, in the online version, at doi:https://doi.org/10.1016/j.epidem.2019.03.006.

References

Alexander, D.J., 2000. A review of avian influenza in different bird species. Vet. Microbiol. 74, 3–13.

Arrêté du 16 novembre 2016, https://www.legifrance.gouv.fr/eli/arrete/2016/11/16/AGRG1633440A/jo/texte.

Arrêté du 31 mars 2017, https://www.legifrance.gouv.fr/affichTexte.do?cidTexte=JORFTEXT000034330812&categorieLien=id.

Bertran, K., Swayne, D.E., Pantin-Jackwood, M.J., Kapczynski, D.R., Spackman, E., Suarez, D.L., 2016. Lack of chicken adaptation of newly emergent Eurasian H5N8 and reassortant H5N2 high pathogenicity avian influenza viruses in the U.S. Is consistent with restricted poultry outbreaks in the Pacific flyway during 2014-2015. Virology 494, 190–197.

Bronner, A., Niqueux, E., Schmitz, A., Le Bouquin, S., Huneau-Salaün, A., Guinat, C., Paul, M., Courcoul, A., Durand, B., 2017. Description de l'épisode d'influenza aviaire hautement pathogène en France en 2016-2017. Bulletin épidémiologique, santé animale et alimentation, vol. 79.

Brown, I., Mulatti, P., Smietanka, K., Staubach, C., Willeberg, P., Adlhoch, C., Candiani, D., Fabris, C., Zancanaro, G., Morgado, J., Verdonck, F., 2017. Avian influenza overview October 2016–August 2017. Efsa J. 15.

Cauchemez, S., Ferguson, N.M., 2012. Methods to infer transmission risk factors in complex outbreak data. J. R. Soc. Interface 9, 456–469.

Chis Ster, I., Ferguson, N.M., 2007. Transmission parameters of the 2001 foot and mouth epidemic in Great Britain. PLoS One 2, e502.

Delpont, M., Blondel, V., Robertet, L., Duret, H., Guerin, J.-L., Vaillancourt, J.-P., Paul, M.C., 2018. Biosecurity practices on foie gras duck farms, Southwest France. Prev. Vet. Med. 158, 78–88.

Eaufrance website, 2011, http://oai.eau-adour-garonne.fr/oai-documents/59656/GED_00000001.pdf.

Ferguson, N.M., Donnelly, C.A., Anderson, R.M., 2001. Transmission intensity and impact of control policies on the foot and mouth epidemic in Great Britain. Nature 413, 542–548.

French Ministry of Agriculture website, 2018, http://agreste.agriculture.gouv.fr/IMG/pdf/R7518A28.pdfhttp://agreste.agriculture.gouv.fr/IMG/pdf/R7518A27.pdf.

Gelman, A., Carlin, J.B., Stern, H.S., Dunson, D.B., Vehtari, A., Rubin, D.B., 2014. Bayesian Data Analysis. CRC Press, Boca Raton.

Gilks, W.R., Richardson, S., Spiegelhalter, D.J., 1996. Markov Chain Monte Carlo in Practice. Chapman and Hall, London, UK.

Guinat, C., Nicolas, G., Vergne, T., Bronner, A., Durand, B., Courcoul, A., Gilbert, M., Guérin, J.-L., Paul, M.C., 2018. Spatio-temporal patterns of highly pathogenic avian influenza virus subtype H5N8 spread, France, 2016 to 2017. Eurosurveillance 23.

Keeling, M.J., Woolhouse, M.E., Shaw, D.J., Matthews, L., Chase-Topping, M., Haydon, D.T., Cornell, S.J., Kappey, J., Wilesmith, J., Grenfell, B.T., 2001. Dynamics of the 2001 UK foot and mouth epidemic: stochastic dispersal in a heterogeneous landscape. Science 294, 813–817.

Le Menach, A., Vergu, E., Grais, R.F., Smith, D.L., Flahault, A., 2006. Key strategies for reducing spread of avian influenza among commercial poultry holdings: lessons for transmission to humans. Proc. Biol. Sci. 273, 2467–2475.

Peiris, J.S., de Jong, M.D., Guan, Y., 2007. Avian influenza virus (H5N1): a threat to human health. Clin. Microbiol. Rev. 20, 243–267.

Smith, G.J., Bahl, J., Vijaykrishna, D., Zhang, J., Poon, L.L., Chen, H., Webster, R.G., Peiris, J.S., Guan, Y., 2009. Dating the emergence of pandemic influenza viruses. Proc. Natl. Acad. Sci. U. S. A. 106, 11709–11712.

Spekreijse, D., Bouma, A., Koch, G., Stegeman, J.A., 2011. Airborne transmission of a highly pathogenic avian influenza virus strain H5N1 between groups of chickens quantified in an experimental setting. Vet. Microbiol. 152, 88–95.

Van De Wiele, A., Humeau, A., Bronner, A., Guillemain, M., Le Loc'h, G., Guérin, J.-L., Cauchard, J., Mercier, A., Calavas, D., 2017. Épisode H5N8 d'influenza aviaire en France en 2016-2017 : quel rôle pour la faune sauvage? Bulletin épidémiologique, santé animale et alimentation 79, 27–31.

Walker, P.G., Cauchemez, S., Metras, R., Dung do, H., Pfeiffer, D., Ghani, A.C., 2010. A Bayesian approach to quantifying the effects of mass poultry vaccination upon the spatial and temporal dynamics of H5N1 in Northern Vietnam. PLoS Comput. Biol. 6, e1000683.

Walker, P., Cauchemez, S., Hartemink, N., Tiensin, T., Ghani, A.C., 2012. Outbreaks of H5N1 in poultry in Thailand: the relative role of poultry production types in sustaining transmission and the impact of active surveillance in control. J. R. Soc. Interface 9, 1836–1845.